TÜBİTAK

Research Article

An innovative peak detection algorithm for photoplethysmography signals: an adaptive segmentation method

Ahmet Reşit KAVSAOĞLU[1,*], Kemal POLAT[2], Mehmet Recep BOZKURT[3]

[1]Department of Biomedical Engineering, Faculty of Engineering, Karabuk University, Karabuk, Turkey
[2]Department of Electrical and Electronics Engineering, Faculty of Engineering and Architecture,
Abant Izzet Baysal University, Bolu, Turkey
[3]Department of Electrical and Electronics Engineering, Faculty of Engineering, Sakarya University, Sakarya, Turkey

Abstract: The purpose of this paper is twofold. The first purpose is to detect M-peaks from raw photoplethysmography (PPG) signals with no preprocessing method applied to the signals. The second purpose is to estimate heart rate variability (HRV) by finding the peaks in the PPG signal. HRV is a measure of the fluctuation of the time interval between heartbeats and is calculated based on time series between strokes derived from electrocardiogram (ECG), arterial pressure (AP), or PPG signals, separately. PPG is a method widely used to measure blood volume of tissue on the basis of blood volume change in every heartbeat. In the estimation of the HRV signal from the PPG signal, HRV is calculated by measuring the time intervals between the peak values in the PPG signal. In the present paper, a novel peak detection algorithm was developed for PPG signals. Finding peak values correctly from PPG signals, the HRV signal can be estimated. This peak detection algorithm has been called an adaptive segmentation method (ASM). In this method, the PPG signals are first separated into segments with sample sizes and then the peak points in these signals are detected by comparing with maximum points in these segments. To evaluate the estimated pulse rate and HRV signals from PPG, Poincaré plots and time domain features including minimum, maximum, mean, mode, standard deviation, variance, skewness, and kurtosis values were used. Our experimental results demonstrated that ASM could be even used both in the estimation of HRV signals and to detect the peaks from raw and noisy PPG signals without a pre-processing method.

Key words: Peak detection, heart rate variability, photoplethysmography signal, adaptive segmentation method

1. Introduction

Photoplethysmography (PPG) is a noninvasive, electro-optical method that provides information about the volume of blood flowing in a test region close to the skin of a body. PPG is obtained by illuminating the region of interest of the body using reflected or transmitted light. In obtaining a PPG signal, the wavelength λ of a light source on one side is placed in a protrusion, for example the finger and a photodetector are placed on the other side of the source to capture the transmitted light. A typical PPG signal consists of the large DC component caused by skin, muscle, and bone not involving blood vessels; a small AC component occurred in the blood vessels leaving from skin, muscle, and bone; and heartbeat frequency components occurred from passing light into arterial blood vessels. A typical PPG signal is composed of S-M-P-Q points and the M point is the peak value in the PPG signal. In the estimation of the heart rate variability (HRV) signal from the PPG

signal, HRV is calculated by computing the time intervals between the M-M (peak values) in the PPG signal. Figure 1 shows the typical PPG signal and its characteristics. Figure 2 presents the schematic representation of transmission and reflected sensors on a finger-type PPG sensor [1]. To date, PPG has been used for determining many physiologic parameters such as oxygen saturation [2], heartbeat, respiration [3], and blood pressure [4] in blood [5]. In addition, PPG also reflects some other important cardiovascular parameters such as vascular occlusion [6]. In the acquisition process of the PPG signal, such sources of noise as motion artifacts, baseline drift, and light noise buried in the PPG signal occur. These noisy components have to be removed before the PPG signal is used for data processing in the detection of heart rate.
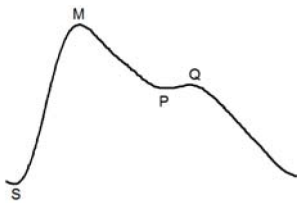

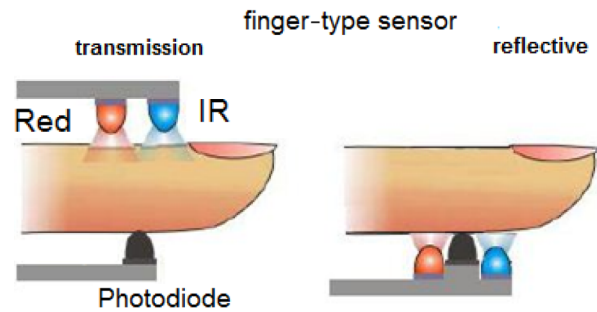**Figure 1.** A sample PPG signal and its characteristic points.

Figure 2. The schematic representation of transmission and reflected sensors on finger-type PPG sensor [19].

The measurement of HRV is of vital significance with respect to health status information, which is used in many medical or sport applications such as stress tests or life-threatening situation prediction [7]. HRV is described as the variation in M-wave intervals (M-M) in PPG signals [8]. There is a high correlation between the RR intervals obtained from ECG signals and peak to peak intervals obtained from PPG signals and this information is verified by many studies [9–11].

In the related literature, there are some peak detection algorithms for PPG signals. Sun et al. [12] emphasized that many vital physiological characteristics are embedded in PPG. They mentioned that of these features heartbeat is the most important for physiological observations in clinical and mobile health services. They proposed a signal processing method on the basis of multiscale data analysis using empirical mode decomposition (EMD) for extracting the heartbeat correctly. They obtained a rate of 84.68% with improving the detection accuracy of heart rate using the signals from the PhysioNet database and their own lab experiment. Liu et al. [13] mentioned that PPG is a suitable noninvasive method for extracting the heart rate on monitoring of physical cases. They emphasized that PPG could be easily corrupted by various effects such as raising or lowering of the hand, breathing, and cardiovascular diseases and therefore the determination of heart rate was a difficult problem. In their work, they proposed a heart rate determination algorithm having better performance than other methods using wavelet and correlation methods. They used the fuzzy logic discriminator to extract the accuracy of each peak in the slope of the PPG signal. Ellenby et al. [14] emphasized that heartbeat detection algorithms had many clinic applications such as pulse oximetry, cardiac arrhythmia detection, and heartbeat monitoring. They designed an automatic detection algorithm determining the place of the first peak following each heartbeat for pressure signals. This algorithm integrated a filter bank with variable cut-off frequency, the heart rate spectral estimation, rank-order nonlinear filters, and the logic of the decision. In their experiments, they obtained a sensitivity of 99.36% and a positive detection rate of 98.43%. Shin et al. [15] mentioned that PPG-based temporal analyses were widely used as an analytical method for the diagnosis of physiological and

cardiovascular diseases. They emphasized that many of the temporal approaches of PPG were based on peak points. The aim of their work was to develop an improved peak detection algorithm in PPG waveforms.

M points (peak points) in PPG signals must be correctly detected in the calculation of the heart rate and HRV from PPG signals. In this study, the detection of M points from raw PPG signal directly will reduce the calculation time in the estimation of HRV from raw PPG signals since no pre-processing method is used. For this reason, a novel method named adaptive segmentation has been proposed to detect the M points from raw PPG signals. In this paper, a novel heartbeat detection algorithm to estimate the heart rate from PPG signals was proposed that involves separating PPG signals into segments with specific sizes, and then detection of peak points in these signals by comparing with maximum points in these segments.

2. Materials

In the present paper, 20 healthy volunteers (15 males and five females, with a mean age of 23.3, a range of 18 to 41, a mean body mass index (BMI) of 22.9, and a range of 17.9 to 29.7) participated in the experiment. The volunteers had no known cardiovascular, neurological, or respiratory diseases. Before the experiment, information was gathered from the volunteers about their physical status, which included height, weight, smoking habit, and BMI. Table 1 gives statistical values of the male and female groups. The volunteers were informed about the study before the data were obtained. The study was approved by the university ethics committee and written informed consent was obtained from all subjects.

Table 1. Descriptive statistics for male and female groups.

Groups	Age (years)	Height (cm)	Weight (kg)	Smoking	Nonsmoking	BMI (kg/m²)
Mean ± SD (range) for males	22.6 ± 6.2 (18–39)	177 ± 5.9 (167–188)	74 ± 10.9 (51–94)	9	6	23.4 ± 3.3 (18.3–29.7)
Mean ± SD (range) for females	25.4 ± 9.7 (19–41)	160 ± 9.7 (147–171)	55 ± 8.1 (47–66)	0	5	21.4 ± 3.4 (17.9–27.8)
Mean ± SD (range) for total	23.3 ± 7.0 (18–41)	173 ± 10.1 (147–188)	69 ± 13.1 (47–94)	9	11	22.9 ± 3.5 (17.9–29.7)

In PPG signal measurements, the SDPPG PPG data acquisition card made by APMKorea (South Korea) was used. This card has a 12-bit ADC and a sampling frequency of 2 kHz. Experiments were carried out in the sitting position with a sampling frequency of 2 kHz over 1 min. The PPG signals obtained from the 20 subjects were recorded on a PC. Figure 3 demonstrates a sample PPG signal of a healthy person recorded during 10 s of a 1-min recording. In this sample PPG signal, there are baseline drift, noise, and motion artifacts.

In addition to the PPG data acquisition card, we used other PPG signals taken from the data including 3189288 and 3189849 signals of the MIMIC II Waveform Database [16], version 3 part l (mimic2wdb/31). These PPG signals were sampled at 125 Hz over 5 min. Figure 4 demonstrates a sample PPG signal during a 10-s section of 5 min recorded in the MIT MIMIC II PPG database [16].

3. Adaptive segmentation algorithm for detecting peaks from PPG signals

The heartbeat could be estimated by measuring the time between the peak intervals in the PPG signal. A sample PPG signal comprises four characteristic points: S, M, P, and Q.
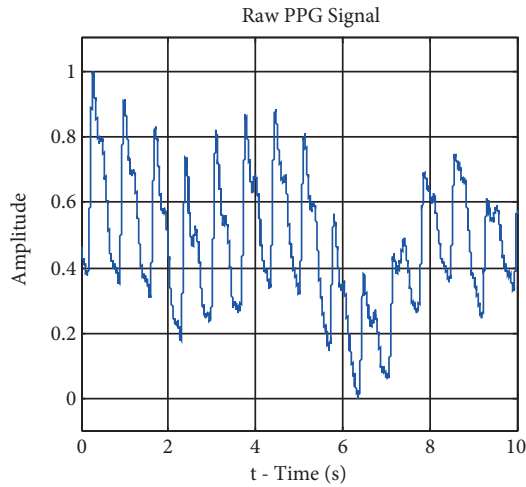
Figure 3. PPG signal of a healthy person recorded during 10 s of 1-min recording (the y-axis is the normalized amplitude in the range of 0 and 1).
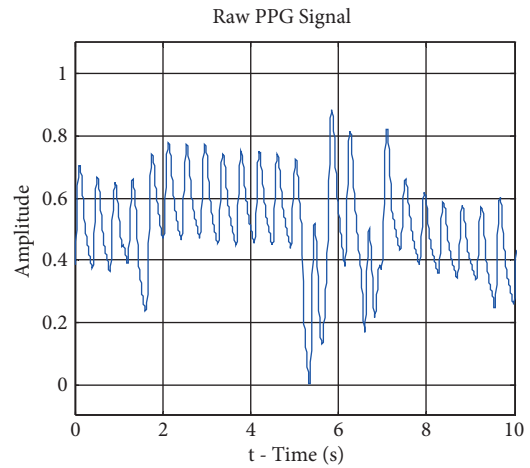
Figure 4. A sample PPG signal during a 10-s section of 5 min recorded in MIT MIMIC II PPG database (the y-axis is the normalized amplitude in the range of 0 and 1) [16].

In this paper, a novel peak detection algorithm for PPG signals is proposed. In this method, the PPG signals were first separated into segments with sample sizes and then the peak points in these signals were detected by comparing with maximum points in these segments. If the maximum point in any segment is less than the maximum value in the segment that comes after it, this signal will have a positive slope. In the reverse situation, if the maximum point in a segment is greater than the maximum value in the segment that comes after it, this signal will have a negative slope. During the transition from a positive slope to a negative slope, the maximum value in the segment with the latest positive slope is considered to be the peak value in that signal. The PPG signal demonstrated in Figure 1 was separated into segments as shown in Figure 5. The transition from a positive slope to a negative slope is shown within segments of S3–S4 and S7–S8 in Figure 5. In these transitions, the maximum values within S3 and S7 segments with the latest positive slope are detected as M and Q points in the PPG signal.
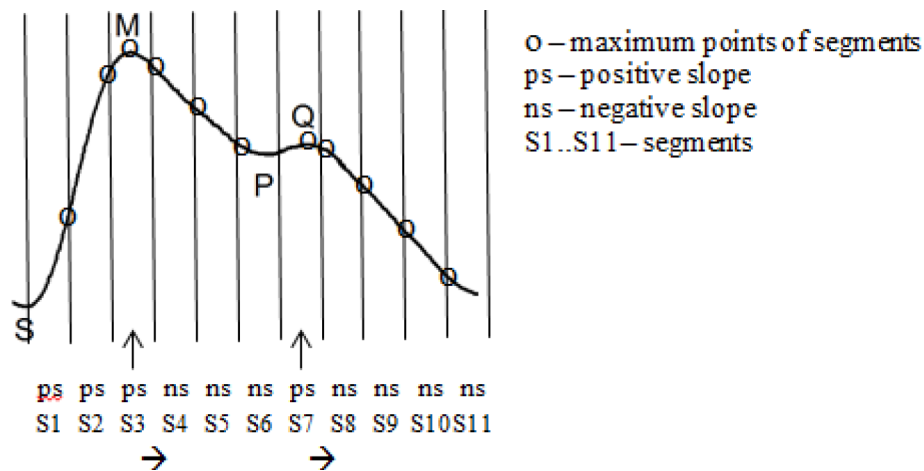

Figure 5. Detection of peak points by separating PPG signal with segments.

The peak number detected in the signal changes depending on the size of the segment. When the segment size is kept very small, all the peaks including peaks that resulted from noise in the signal can be detected.

When the segment size is kept very large, M peaks cannot be detected. For instance, two peak points in the PPG signals were detected with 5 segments shown in Figure 6a. Four peak points in the PPG signals were detected with 16 segments shown in Figure 6b. Normally, there are two peak points in the PPG signals as shown in Figure 6. The selection of segment size should be adjusted adaptively. Therefore, the segment size must be within the range of the minimum and maximum values. In the proposed algorithm, the range value of maximum and minimum segment sizes calculated depending on maximum and minimum heartbeat values for humans was used as a criterion.

a) Two peaks detected in PPG signals by optimum segment points (correct estimation).

b) Four peaks detected in PPG signals by big segment points (wrong estimation).

Figure 6. Peak points detected according to chosen sample segment points.

In order to find peaks in PPG signals, according to the adaptive segmentation method capable of finding the most suitable segment size proposed in this study, an unknown heart rate period should be chosen in at least three segments. Figure 7 shows the separating of the heartbeat period into at least three segments. The reason for establishing at least three segments within a given heartbeat period is to detect the positive and negative slopes that take place within this period. If fewer than three segments are created in the heartbeat period, M peak points will not be detected.
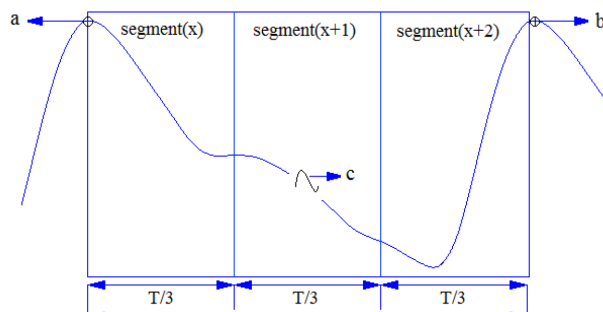

Figure 7. Separating a given heartbeat period into three segments where a and b points show the peak points to be detected and c point represents the noise and/or the peaks outside M peak points.

The noise or unwanted peaks replaced in the segments are blinked in the proposed method. The peak values (M peaks) could be properly detected with the proposed adaptive segmentation method without a preprocessing method including noise elimination, moving average, filtering etc. In the proposed method, firstly the minimum segment size is obtained when the heartbeat period is divided by three in the maximum heart rate. Then heart rate begins to be perceived in the peaks with a minimum segment size. From the peaks

detected in the PPG signals, M-M time intervals for the PPG signal are calculated. The standard deviation and average heart rate values are computed from the peak to peak time interval arrays. Then the peaks are again detected magnifying the sampling frequency at the rate of 1% and standard deviation and average heart rate are calculated. In this way, the calculation of standard deviation and mean heart rate continues until the maximum segment size is found by dividing the heartbeat period into three in the minimum heart rate.
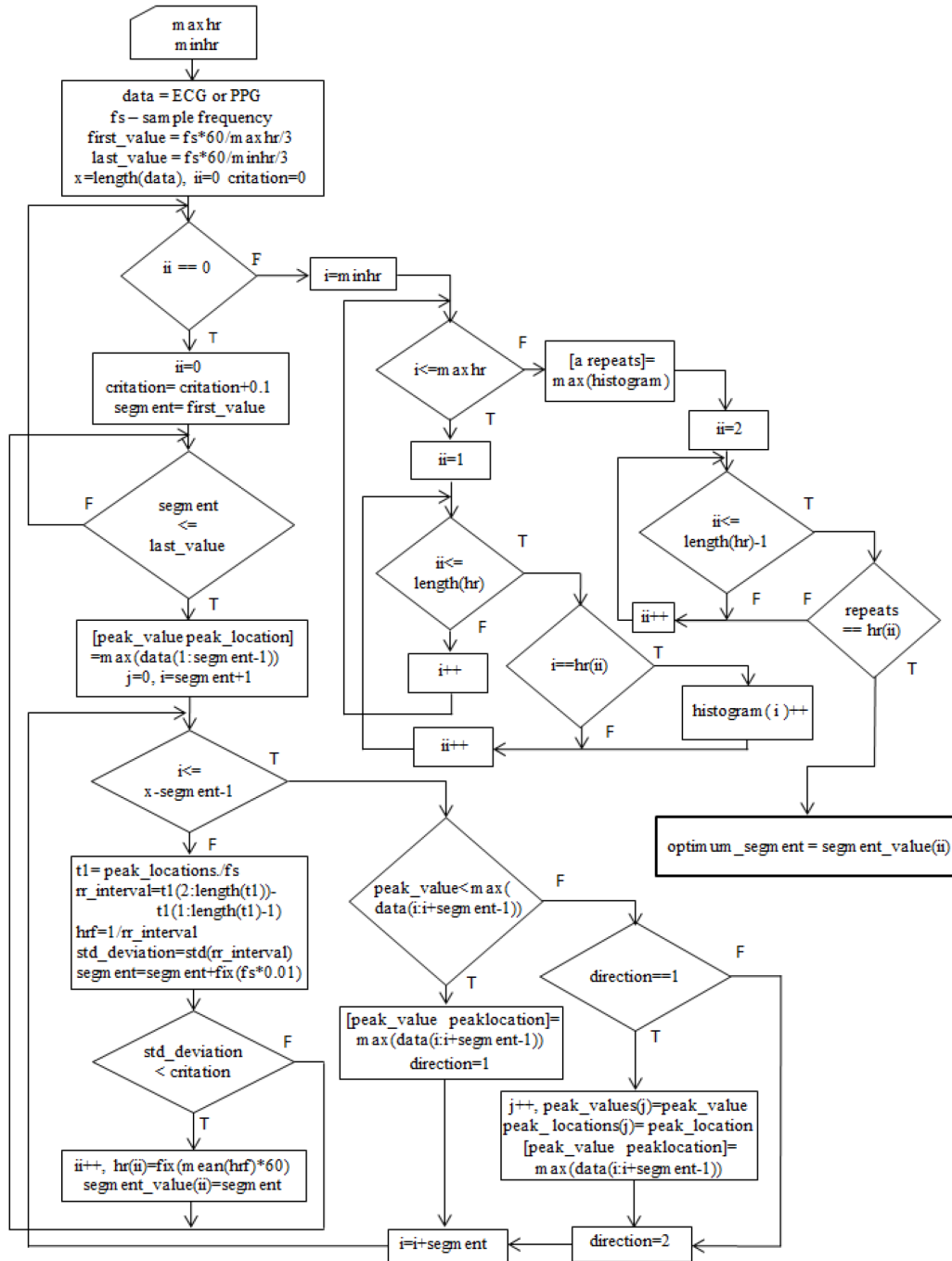
Figure 8. The algorithm for finding the optimum segment size.

The HRV and its histogram for heart rate values less than 0.1 of standard deviation from average calculated according to segment size depending on segment size taken into account are calculated and drawn. In this point, the standard deviation value was used as a threshold. In this way, the peaks detected depending on segment size will have the same pulse period by determining a threshold. If the standard deviation from average heart rate values calculated according to segment size is less than 0.1, the size of the segment will be increased by 0.1 at a step every time and HRV and its histogram will be calculated and drawn. For heartbeat values with the highest repeat numbers in the histogram, the segment size is taken as the optimal segment size. Finally, for the optimum segment size, the detected peaks will be the M peaks for the PPG signal. Figure 8 shows the flowchart of the algorithm created for finding the optimum segment size in the proposed adaptive segmentation method. Figure 9 presents the flowchart of the peak detection algorithm using optimum segment size.
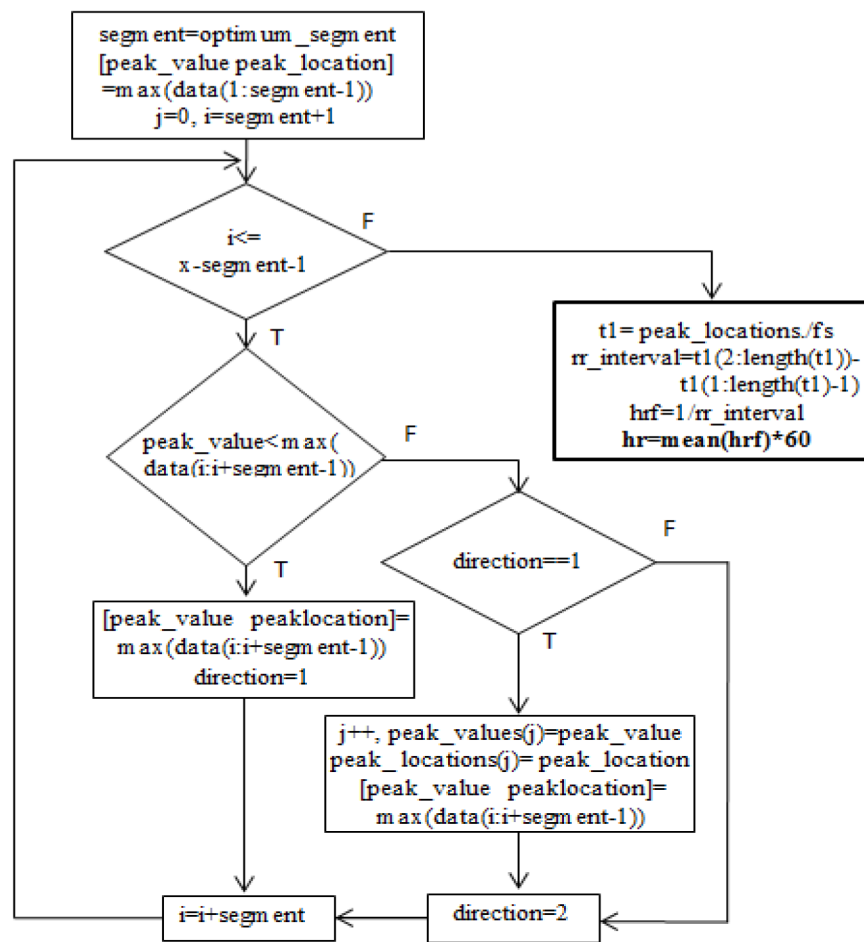

Figure 9. The peak detection algorithm using optimum segment size.

4. Results and discussion

The purpose of this paper is twofold. The first purpose is to detect the peak from raw PPG signals without applying any pre-processing method to the signals. The second purpose is to estimate HRV by finding the peaks in the PPG signal. In obtaining PPG signals, two different PPG signals were used and taken from MIT-MIMIC II database [16] and the PPG data acquisition board made by APMKorea. The PPG signals used in the

experimental results were obtained from the SDPPG PPG data acquisition card below (South Korea). Figure 10 presents peak detection results based on the ASM and the fixed segment size (40 and 800 segments) using the raw and pre-processed PPG signals. In the fixed segment size method, a fixed segment number including 40 and 800 was applied to the raw PPG signal. As can be seen from Figures 10b and 10c, the fixed segment size method could not find the peaks of the raw PPG signal. Figure 10d presents the M peaks found in the pre-processed PPG signal by MA using ASM, Figure 10e shows the M peaks found in the pre-processed PPG signal by MA combined with ASM, and Figure 10f denotes the M peaks found in the pre-processed PPG signal by FIR low pass filter ($f_c = 10$ Hz) using ASM. The ASM was able to accurately find the peak values in both raw and pre-processed PPG signals.

Figure 11 shows the HRV signals estimated according to peak values time interval series from the raw and pre-processed PPG signals. Three HRV graphics have been obtained with ASM (first), fixed segment size (40 segment size), and fixed segment size (800 segment size), respectively. As can be seen from the HRV graphics, since the fixed point segment sizes were not suitable for finding the peaks in PPG signals, the obtained HRV graphics were not correct. Therefore, the best and truest HRV graphic is with ASM.

Poincaré plots are drawn for the two signals: MM intervals derived. These plots are useful visualization tools to present the compatibility of all the HRV signals. While a Poincaré plot with all the data points clustered together produces a good quality HRV signal, the Poincaré plot with the scattered data points produces corrupted HRV signals [17,18]. Figure 12 shows Poincaré plots obtained from the raw and pre-processed PPG signals. The Poincaré plots showed that the data in the obtained Poincaré plots for fixed point segment sizes (40 and 800) were not collected together, while the data in the obtained Poincaré plot for ASM were collected together.

All the PPG signals were analyzed using MATLAB 7.6 software. To evaluate the estimated HRV signals from the PPG, the Poincaré plots and time domain features including minimum, maximum, mean, mode, standard deviation, variance, skewness, and kurtosis values were used. Table 2 gives the time domain features of HRV signals obtained by processing of PPG signals taken from 20 healthy people using a SDPPG data acquisition card at a sampling frequency of 2 kHz. Table 2 allows the possibility of comparing the values obtained. The skewness and kurtosis measures give information to us about the distribution of HRV in Table 2.

In the HRV distribution obtained by ASM with and without pre-treatment, skewness close to zero, unity, and greater than unity indicates the concentration of the distribution around the mean HR, the case of constant segment dimensions, and the aggregation of HR distribution below the mean, respectively. High and low kurtosis values show low and high variability in HRV.

Table 3 gives the pulse rate values estimated using an adaptive segmentation method in raw PPG signals. In Table 3, SpO_2 denotes the oxygen saturation value of a healthy person using a pulse oximeter device; PRbpm shows pulse rate per minute of a healthy person. In this table, we have also given the oxygen saturation level and heart rate measured by a pulse oximeter device and compared them with estimated pulse rates by ASM. The obtained results demonstrated that the proposed ASM could be surely used for both detecting peaks and estimating the pulse rate from raw PPG signals without any signal processing methods.

Table 4 shows results obtained using the MIT MIMIC II database (mimic2wdb/31) 3189288/PLETH signal [16]. To show the superiority of the proposed ASM, we have also used PPG signals belonging to the MIT MIMIC II database [16]. The experimental results showed that the ASM could correctly detect the peaks in raw PPG signals without any signal pre-processing methods such as noise elimination, baseline wandering, and moving average.
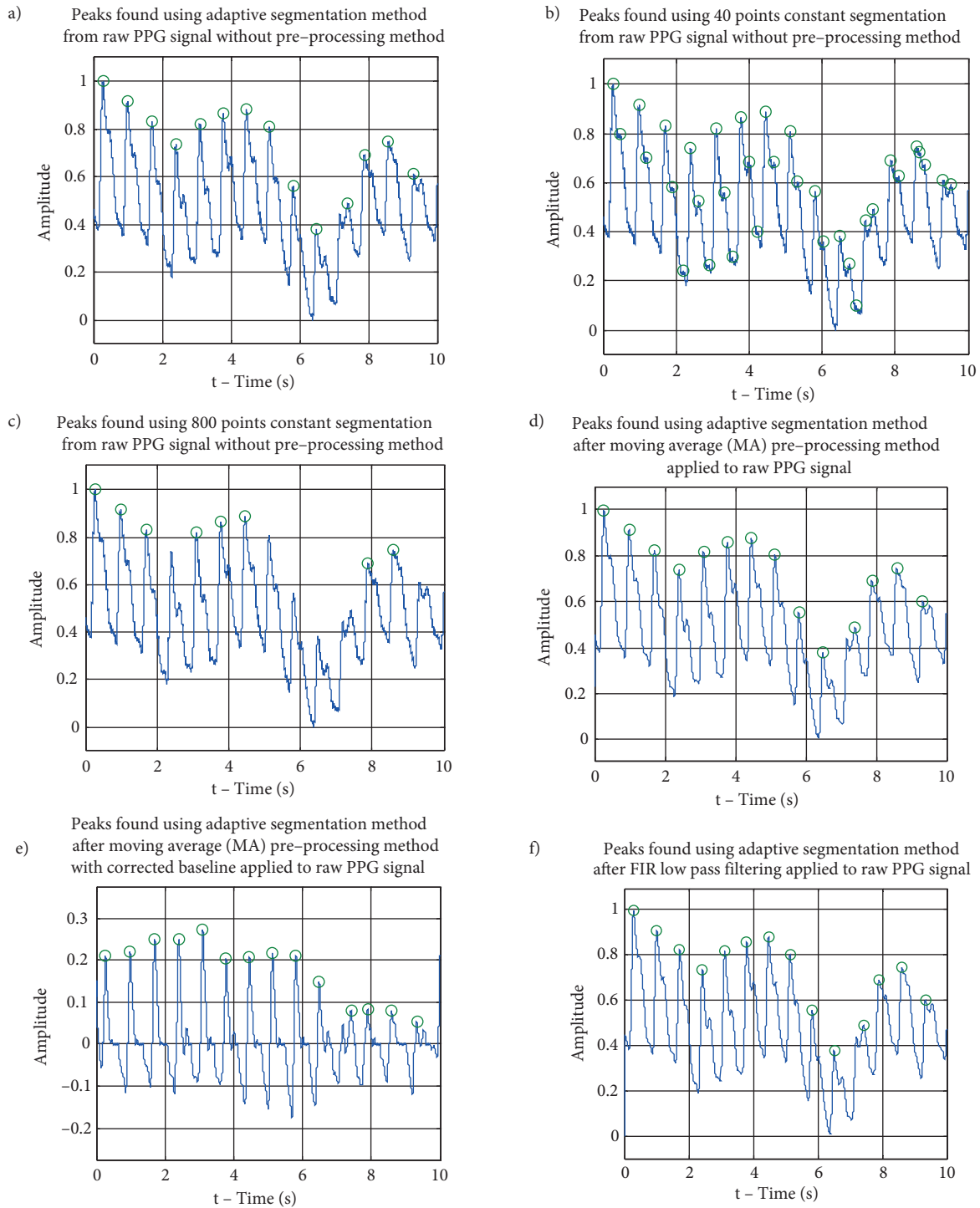
Figure 10. Comparison of peaks found in raw PPG signals using an adaptive segmentation method (ASM): (a) M peaks found in raw PPG signals using ASM, (b) M peaks found in raw PPG signals using a fixed segment size (the point number: 40), and (c) M peaks found in raw PPG signals using a fixed segment size (the point number: 800), (d) the M peaks found in pre-processed PPG signal by MA using ASM, (e) the M peaks found in pre-processed PPG signal by MA combined with using ASM, (f) the M peaks found in pre-processed PPG signal by FIR low pass filter ($f_c = 10$ Hz) using ASM.
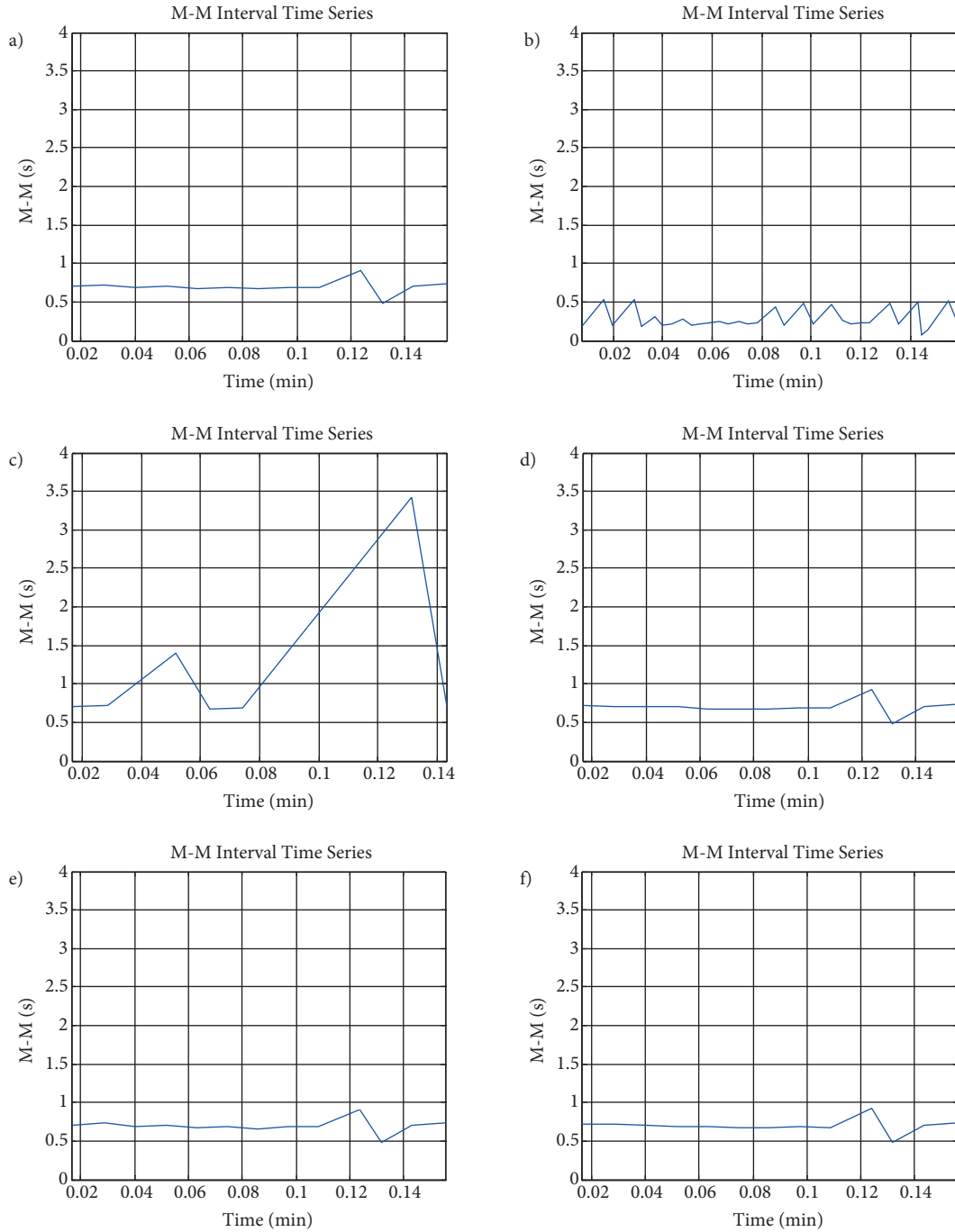
Figure 11. HRV signals estimated according to peak points time interval series from raw PPG signals: (a) HRV signals estimated in raw PPG signals with ASM, (b) HRV signals estimated in raw PPG signals using a fixed segment size (the point number: 40), and (c) HRV signals estimated in raw PPG signals using a fixed segment size (the point number: 800), (d) the HRV signal estimated in pre-processed PPG signal by MA method, (e) the HRV signal estimated in pre-processed PPG signal by MA combined with baseline wandering, (f) the HRV signal estimated in pre-processed PPG signal by FIR low pass filter (f_c = 10 Hz).
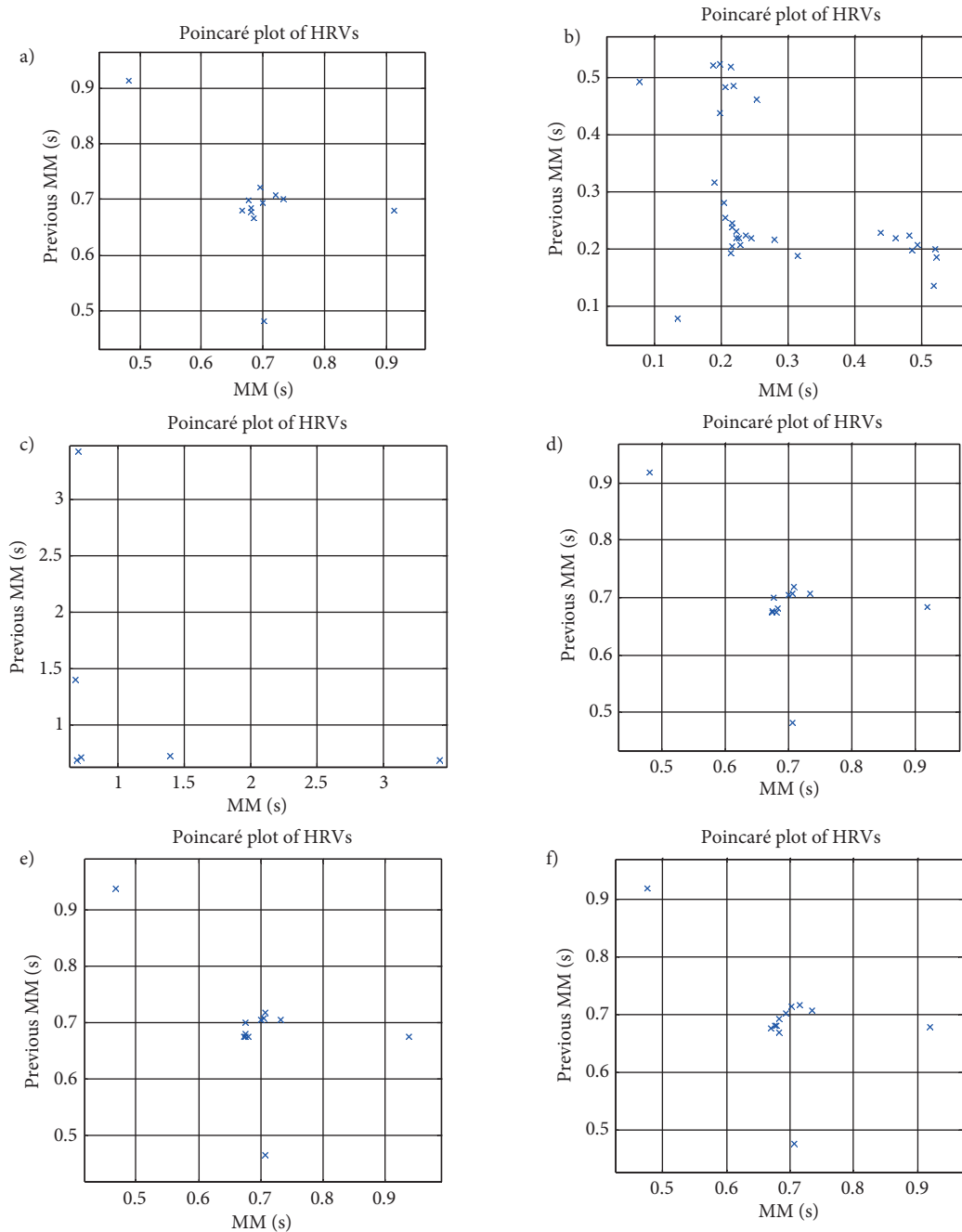
Figure 12. Poincaré plots obtained from raw PPG signals: (a) Poincaré plot obtained from raw PPG signals with ASM, (b) Poincaré plot obtained from raw PPG signals using a fixed segment size (the point number: 40), and (c) Poincaré plot obtained from raw PPG signals using a fixed segment size (the point number: 800), (d) the obtained Poincaré plot in pre-processed PPG signal by MA method, (e) the obtained Poincaré plot in pre-processed PPG signal by MA combined with baseline wandering, (f) the obtained Poincaré plot in pre-processed PPG signal by FIR low pass filter ($f_c = 10$ Hz).

ASM results obtained from the PeakFinder algorithm (http://www.mathworks.com/matlabcentral/fileexchange/25500-peakfinder) over a 30-s PPG signal for the comparison of performance of the proposed method are presented in Figure 13. To compare our method with other peak detection algorithms, we used

Table 2. Time domain features of HRV signals obtained by processing of PPG signals taken from 20 healthy people using a SDPPG data acquisition card at a sampling frequency of 2 kHz.

Time domain features	In HRV signals obtained from raw PPG signals (with 300 segments found optimally by ASM)	In HRV signals obtained from raw PPG signals using fixed segment size (40 points)	In HRV signals obtained from raw PPG signals using fixed segment size (800 points)	In the HRV signal obtained from pre-processed PPG signal by MA method	In the HRV signal obtained from pre-processed PPG signal by MA combined with baseline wandering method	In the HRV signal obtained from pre-processed PPG signal by FIR low pass filter (cutoff frequency = 10 Hz)
Min MM (s)	0.7418	0.2362	0.7592	0.7568	0.7304	0.7577
Max MM (s)	0.8929	0.8101	1.5432	1.5468	1.4156	1.5650
Mean MM (s)	0.8142	0.5057	1.0061	1.0086	0.9789	0.9938
Mode MM (s)	0.7566	0.2801	0.7631	0.7568	0.7344	0.7608
Stand Dev (s)	0.0480	0.1699	0.3049	0.3099	0.2601	0.3114
Variance	0.0030	0.0388	0.1749	0.1777	0.1394	0.1890
Skewness	0.1747	0.1137	0.6535	0.5937	0.4074	0.6518
Kurtosis	2.4880	2.8548	2.8016	2.5684	2.4063	2.7116

Table 3. Pulse rate values estimated using an adaptive segmentation method in raw PPG signals.

Subject	Values found by a pulse oximeter device		The used and obtained parameters belonging to the raw PPG signal				
	SpO$_2$	PRbpm	PRbpm	The difference between actual PRbpm and estimated PRbpm	Segment point number found optimally by ASM	Standard deviation values	The detection accuracy of ASM algorithm
1	94	73	72.20	0.8	260	0.0326	98.90
2	97	87	87.70	0.7	320	0.0896	99.20
3	97	92	91.27	0.73	260	0.0185	99.21
4	98	96	96.49	0.49	280	0.0177	99.49
5	98	82	81.60	0.4	260	0.0318	99.51
6	98	60	58.99	1.01	300	0.0589	98.32
7	98	63	61.47	1.53	300	0.0943	97.57
8	96	97	96.73	0.27	260	0.0745	99.72
9	98	58	59.51	1.51	260	0.0928	97.40
10	97	57	57.86	0.86	260	0.0684	98.49
11	98	67	67.66	0.66	260	0.0360	99.01
12	97	87	86.88	0.12	260	0.0345	99.86
13	98	79	78.37	0.63	260	0.0323	99.20
14	98	71	70.92	0.08	260	0.0212	99.89
15	98	68	69.37	1.37	260	0.0469	97.99
16	96	70	70.98	0.98	360	0.0955	98.60
17	97	74	75.04	1.04	380	0.0266	98.59
18	96	87	87.69	0.69	260	0.0278	99.21
19	98	68	67.14	0.86	260	0.0377	98.74
20	98	80	80.16	0.16	260	0.0230	99.80
Average	97.25	75.8	75.9	0.744	279	0.04803	98.93

the PeakFinder algorithm. Normally, the example raw PPG signal has 35 M peaks. While our method finds all peaks including 35 M peaks, the PeakFinder algorithm finds 48 peaks (13 unwanted peaks in PPG signal). The PeakFinder algorithm and ASM complete their operation in 0.294 s and a shorter time of 0.271 s, respec-

Table 4. Time domain features of HRV signals obtained processing PPG signals taken from MIT MIMIC II database (mimic2wdb/31) 3189288 PPG signals at a sampling frequency of 125 Hz (recording time: 300 seconds).

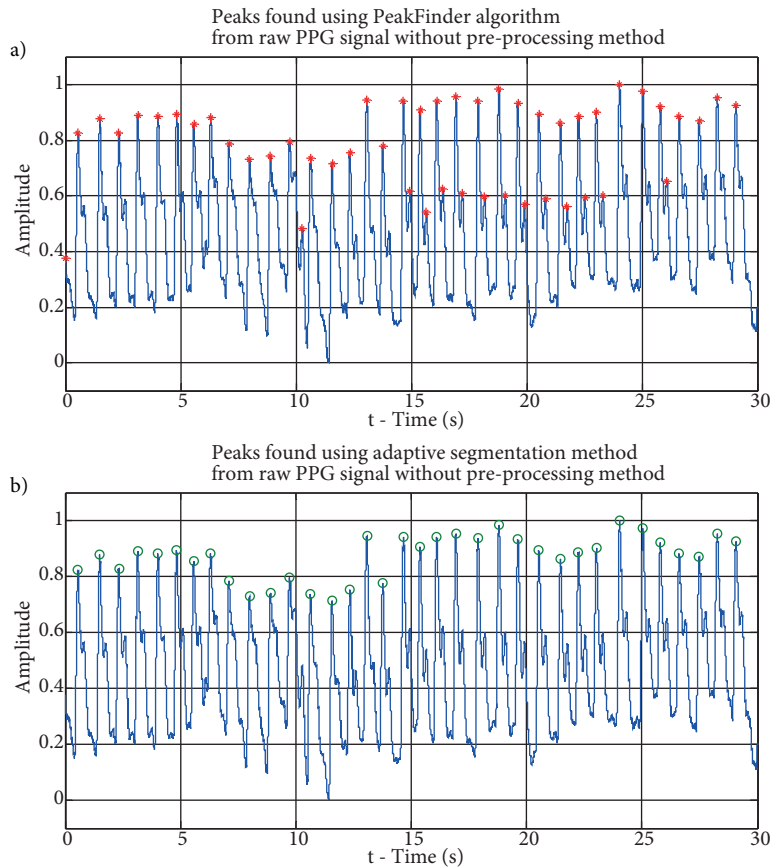| Time domain features	In HRV signals obtained from raw PPG signals (with 12 segments found optimally by ASM)	In HRV signals obtained from raw PPG signal using a fixed segment size (4 points)	In HRV signals obtained from raw PPG signal using a fixed segment size (25 points)
Min MM (s)	0.3200	0.1120	0.3280
Max MM (s)	0.9520	0.8960	1.6400
Mean MM (s)	0.4246	0.4090	0.4774
Mode MM (s)	0.4240	0.4160	0.4160
Stand Dev (s)	0.0444	0.0639	0.1726
Variance	0.0020	0.0041	0.0298
Skewness	8.7681	–0.9362	3.3709
Kurtosis	95.6888	17.7748	15.4072
PRbpm	141.309	146.699	125.68

Figure 13. Comparison of peak detection algorithms including PeakFinder and ASM methods: a) the found peaks from PPG signal using PeakFinder algorithm b) the found peaks from PPG signal using the proposed ASM algorithm.

tively. Moreover, ASM operates without the need for a threshold level, as with the conventional peak-detection algorithms. These results show that the proposed ASM appears to be promising for sensing peaks of PPG signals.

5. Conclusions

In the present experimental study involving 20 volunteers using the SDPPG data acquisition card and MIT-MIMIC II public database, the ASM algorithm was proposed and tested both to estimate the HRV values and to detect peaks in the PPG signals. The PPG signals used included noises such as analogue circuit noises, changes in ambient light, and baseline drift caused by respiration and motion artifacts. The proposed ASM led to accurate estimates of HRV and peak values for the raw PPG signals without any signal pre-processing method. Our results showed that the ASM could be even used in the estimation of HRV signals from corrupted and noisy PPG signals without the need for a pre-processing method. Using raw PPG waveforms without a pre-processing method appears to be promising given the digital signal processing cards.

References

[1] Bailey J, Fecteau M, Pendleton NL. Wireless pulse oximeter. Bachelor Degree Thesis, Worcester Polytechnic Institute, New York, NY, USA, 2008.

[2] Kyriacou PA, Powell S, Langford RM, Jones DP. Investigation of oesophageal photoplethysmographic signals and blood oxygen saturation measurements in cardiothoracic surgery patients. Physiol Meas 2002; 23: 533-545.

[3] Johansson A. Neural network for photoplethysmographic respiratory rate monitoring. Med Biol Eng Comput 2003; 41: 242-248.

[4] Binns SH, Sisson DD, Buoscio DA, Schaeffer DJ. Doppler ultrasonographic, oscillometric sphygmomanometric, and photoplethysmographic techniques for noninvasive blood-pressure measurement in anesthetized cats. J Vet Intern Med 1995; 9: 405-414.

[5] Allen J. Photoplethysmography and its application in clinical physiological measurement. Physiol Meas 2007; 28: 1-39.

[6] Usman SB, Ali MAB, Reaz MMB, Chellapan K. Second derivative of photoplethysmogram in estimating vascular aging among diabetic patients. In: International Conference for Technical Postgraduates; 14–15 December 2009; Kuala Lumpur, Malaysia: Techpos. pp. 5-7.

[7] Parák J, Havlík J. ECG signal processing and heart rate frequency detection methods. In: 19th Annual Conference on Technical Computing; 2011; Prague, Czech Republic: pp. 91-96.

[8] Akar SA, Kara S, Latifoğlu F, Bilgiç V. Spectral analysis of photoplethysmographic signals: the importance of preprocessing. Biomed Signal Proces 2013; 8: 16-22.

[9] Teng XF, Zhang YT. Study on the peak interval variability of photoplethysmographic signals. In: IEEE EMBS Asian-Pacific Conference on Biomedical Engineering; 20–22 October 2003; Kyoto Osaka Nara, Japan: IEEE EMBS. pp. 140-141.

[10] McKinley PS, Shapiro PA, Bagiella E, Myers MM, De Meersman RE, Grant I, Sloan RP. Deriving heart period variability from blood pressure waveforms. J Appl Physiol 2003; 95: 1431-1438.

[11] Johnston W, Mendelson Y. Extracting heart rate variability from a wearable reflectance pulse oximeter. In: IEEE Proc. of 31st Annual Northeast Bioengineering; 2–3 April 2005; Hoboken, NJ, USA: IEEE. pp. 157-158.

[12] Sun X, Yang P, Li Y, Gao Z, Zhang YT. Robust heart beat detection from photoplethysmography interlaced with motion artifacts based on empirical mode decomposition. In: IEEE-EMBS International Conference on Biomedical and Health Informatics (BHI); 5–7 Jan. 2012; Shenzhen, Hong Kong: IEEE. pp. 775-778.

[13] Liu SH, Chang KM, Fu TH. Heart rate extraction from photoplethysmogram on fuzzy logic discriminator. Eng Appl Artif Intel 2010; 23: 968-977.

[14] Aboy, M, McNames J, Tran Thong, Tsunami D, Ellenby MS, Goldstein B. An automatic beat detection algorithm for pressure signals. IEEE T Bio-Med Eng 2005; 52: 1662-1670.

[15] Shin HS, Lee C, Lee M. Adaptive threshold method for the peak detection of photoplethysmographic waveform. Comput Biol Med 2009; 39: 1145-1152.

[16] Goldberger AL, Amaral LAN, Glass L, Hausdorff JM, Ivanov PCh, Mark RG, Mietus JE, Moody GB, Peng CK, Stanley HE. PhysioBank, PhysioToolkit, and PhysioNet: components of a new research resource for complex physiologic signals. Circulation 2000; 101: 215-220.

[17] Bolanos M, Nazeran H, Haltiwanger E. Comparison of heart rate variability signal features derived from electro-cardiography and photoplethysmography in healthy individuals. In: Proceedings of the 28th IEEE EMBS Annual International Conference; Aug 30–Sept 3 2006; New York, NY, USA: IEEE. pp. 4289- 4294.

[18] Brennam M, Palaniswami M, Kamen P. Do existing measures of poincaré plot geometry reflect nonlinear features of heart rate variability? IEEE T Bio-Med Eng 2001; 48: 1342-1347.

[19] Ateş G, Polat K, Measuring of oxygen saturation using pulse oximeter based on fuzzy logic. In: IEEE MeMeA International Symposium on Medical Measurements and Applications; 18–19 May 2012; 2012; Budapest, Hungary: IEEE. pp. 51-56.